[2]Batchelor, G. K., "Axial Flow in Trailing Line Vortices," *Journal of Fluid Mechanics,* Vol. 20, 1964, pp. 645-658.
[3]Batchelor, G. K., *An Introduction to Fluid Dynamics,* Cambridge, England, 1967, pp. 518-519.
[4]Lofquist, K. E. B., Private communication, 1988.
[5]Landau, L. D. and Lifshitz, E. M., *Fluid Mechanics,* Pergamon Press, London, 1959, pp. 175-176.
[6]Earnshaw, P. B. "An Experimental Investigation of the Structure of a Leading Edge Vortex," Royal Aeronautical Establishment, TN Aero 2740, 1961; Aeronautical Research Council, R&M 3281.
[7]Verhaagen, N. G. and Kruisbrink, A. C. H., "Entrainment Effect of a Leading-Edge Vortex," *AIAA Journal,* Vol. 25, Aug. 1987, pp. 1025-1032.
[8]Chigier, N. A. and Corsiglia, V. R. 1972. "Wind-Tunnel Studies of Wing Wake Turbulence," *Journal of Aircraft*, Vol. 9, Dec. 1972, pp. 820-825.
[9]Kuchemann, D., *The Aerodynamic Design of Aircraft,* Pergamon Press, London, 1978, pp. 393-394.

Structural Optimization for Aeroelastic Control Effectiveness

M. Karpel* and Z. Sheena†
Israel Aircraft Industries, Lod, Israel

Introduction

THE issue of aeroelastic effectiveness of wing trailing-edge control surfaces may present a major design goal for the aircraft designer. A fully stressed and buckling-designed wing is sometimes deficient in meeting the required aircraft performance because of insufficient control effectiveness at high speed. The problem is how to resize the wing structure such that the control effectiveness requirements will be satisfied with minimum increase in weight.

The FASTOP computer program[1,2] applied a simple and efficient method for optimization of metallic structure with strength and flutter constraints. The method was later extended to deal with composite structures subjected to strength and deflection constraints and integrated into the ASOP-3 computer program.[3] Further development of the basic optimization procedure of FASTOP to address constraints on aeroelastic effectiveness and static divergence is given by Lerner and Markowitz[4] and was used in the design of the X-29 forward-swept-wing demonstrator aircraft[5] and on the Lavi wing and vertical tail.[6] The most time-consuming portion of the Ref. 4 procedure is the calculations of the aeroelastic effectiveness parameters after each optimization step. This calculation is performed using a discrete-coordinate approach with the structural model clamped to the ground to allow inversion of the stiffness matrix. As a result, inertia relief effects are not taken into account during the optimization process.

Sheena and Karpel[7] used the modal approach for performing static aeroelastic analysis. The present work follows the formulation of Ref. 7 and extends it to include effectiveness derivative calculations along the optimization path. This application, which uses free-free aircraft vibration modes, allows larger optimization steps between two finite-element model updates and makes the calculations so efficient that a major optimization cycle may be completed in a short online computer session. Another advantage of the present method is that inertia relief effects are implicitly taken into account in calculating the effectiveness parameters and their derivatives.

Received Jan. 25, 1988; revision received Aug. 26, 1988.

*Head, Dynamics and Loads; currently, Senior Research Associate, Department of Aeronautical Engineering, Technion—Israel Institute of Technology, Haifa, Israel.
†Structural Dynamics Engineer.

Aeroelastic Effectiveness

The method of static aeroelastic analysis using aircraft vibration modes is described in Ref. 7. The basic assumption in the modal approach is that the deflections of the structure can be represented as a linear combination of a limited set of vibration mode shapes. When a set of free-free vibration modes is used as generalized coordinates, the aircraft matrix equation of motion can be partitioned into rigid and elastic parts:

$$\begin{bmatrix} M_{rr} & 0 \\ 0 & M_{ee} \end{bmatrix} \begin{Bmatrix} \ddot{\xi}_r \\ \ddot{\xi}_e \end{Bmatrix} + \begin{bmatrix} 0 & 0 \\ 0 & C \end{bmatrix} \begin{Bmatrix} \dot{\xi}_r \\ \dot{\xi}_e \end{Bmatrix} + \begin{bmatrix} 0 & 0 \\ 0 & K_{ee} \end{bmatrix} \begin{Bmatrix} \xi_r \\ \xi_e \end{Bmatrix} = q \begin{bmatrix} R_{rr} & R_{re} \\ R_{er} & R_{ee} \end{bmatrix} \begin{Bmatrix} \xi_r \\ \xi_e \end{Bmatrix} + \begin{Bmatrix} F_r \\ F_e \end{Bmatrix} \tag{1}$$

where $[M]$, $[C]$, and $[K]$ are the diagonal generalized mass, damping, and stiffness matrices, $[R]$ is the generalized aerodynamic force matrix, $\{\xi\}$ is the generalized coordinate displacement vector, and $\{F\}$ is a vector of the generalized external forces which cannot be related to $\{\xi\}$ through a constant coefficient matrix. Subscripts r and e related to rigid-body and elastic modes, respectively, and q is the dynamic pressure. The elements of $[R_{rr}]$ are the rigid aerodynamic coefficients associated with rigid-body displacements. The generalized aerodynamic matrix is calculated by

$$[R] = [\Psi]^T [AFC] [\Psi'] \tag{2}$$

where $[AFC]$ is the aerodynamic force coefficient matrix obtained by a linear panel aerodynamic theory, $[\Psi]$ is the mode shape matrix where displacements are defined at the panel centroids, and $[\Psi']$ are the chordwise derivatives of $[\Psi]$, where slopes are defined at the panel control points. $[\Psi]$ and $[\Psi']$ are obtained from the modal displacements at the structural points by a surface spline routine. When a quasisteady motion is assumed,

$$\{\ddot{\xi}_e\} = \{\dot{\xi}_e\} = \{0\} \tag{3}$$

and Eq. (1) yields

$$[M_{rr}] \{\ddot{\xi}_r\} = q[\bar{R}_{rr}] \{\xi_r\} + \{\bar{F}_r\} \tag{4}$$

where

$$[\bar{R}_{rr}] = [R_{rr}] + q[R_{re}]([K_{ee}] - q[R_{ee}])^{-1} [R_{er}] \tag{5}$$

$$\{\bar{F}_r\} = \{F_r\} + q[R_{re}]([K_{ee}] - q[R_{ee}])^{-1} \{F_e\} \tag{6}$$

The elements of $[\bar{R}_{rr}]$ of Eq. (5) are the "flexibilized" aerodynamic coefficients associated with the aircraft rigid-body displacements. The rigid-body coordinates can be extended to include rigid control surface rotations. In this way, Eq. (5) can be used to flexibilize aerodynamic coefficients such as rolling moment due to aileron deflection (C_{L_δ}) or hinge moment due to aileron deflection (C_{H_δ}). Equation (6) can be used to flexibilize aerodynamic coefficients due to rigid-body velocities. This is done by defining

$$\begin{bmatrix} F_r \\ F_e \end{bmatrix} = q \begin{bmatrix} \Psi_r^T \\ \Psi_e^T \end{bmatrix} [AFC] \{\alpha_i\} \tag{7}$$

where $\{\alpha_i\}$ is the vector of induced-panel angles-of-attack due to the rigid-body velocities.

The aeroelastic effectiveness of an aerodynamic coefficient is defined as

$$\eta_{ij} \equiv \frac{\bar{R}_{rr_{ij}}}{R_{rr_{ij}}} = 1 + \frac{q}{R_{rr_{ij}}} \{R_{re_i}\}^T ([K_{ee}] - q[R_{ee}])^{-1} \{R_{er_j}\} \tag{8}$$

where $\{R_{re_i}\}^T$ and $\{R_{er_j}\}$ are the ith row and the jth column of $[R_{re}]$ and $[R_{er}]$, respectively.

Effectiveness Derivatives

It is assumed that the weight of a structural element w_k is

proportional to its stiffness. So,

$$\frac{\partial[K]}{\partial w_k} = \frac{[K^{(k)}]}{w_k} \tag{9}$$

where $[K]$ is the full stiffness matrix in discrete coordinates and $[K^{(k)}]$ is a zero matrix except for the terms associated with the kth element. $[K]$ is related to the generalized stiffness matrix by

$$[K_{ee}] = [\Phi_e]^T[K][\Phi_e] \tag{10}$$

where $[\Phi_e]$ is the elastic mode shape matrix where displacements are defined at the structural grid points. It is also assumed that the additional material due to resizing has negligible effect on inertia relief. Differentiation of Eq. (8) with respect to w_k under these assumptions yields

$$\frac{\partial \eta_{ij}}{\partial w_k} = -\frac{q}{R_{rr_{ij}} w_k} \{R_{re_i}\}^T[B]^{-1}[K_{ee}^{(k)}][B]^{-1}\{R_{er_j}\} \tag{11}$$

where

$$[B] = [K_{ee}] - q[R_{ee}] \tag{12}$$

and $[K_{ee}^{(k)}]$ is the contribution of the kth element to $[K_{ee}]$.

Sometimes, as will be explained in the Numerical Example section, the η value that drives the optimization is defined as the ratio between two effectiveness values. In this case,

$$\frac{\partial \eta}{\partial w_k} \equiv \frac{\partial}{\partial w_k}\left(\frac{\eta_1}{\eta_2}\right) = \left(\eta_2 \frac{\partial \eta_1}{\partial w_k} - \eta_1 \frac{\partial \eta_2}{\partial w_k}\right)\Big/ \eta_2^2 \tag{13}$$

Optimization Process

The purpose of the structural optimization process is to obtain the target effectiveness with a minimum weight increase. A NASTRAN run for vibration modes, which also creates a data base of element contributions $[K_{ee}^{(k)}]$ to the generalized stiffness matrix, is first performed. The generalized aerodynamic matrices of Eq. (1) are then generated using Eq. (2), and effectiveness analysis using Eq. (8) is performed. The most deficient effectiveness parameter η is then chosen for driving a major optimization cycle which aims to meet the required effectiveness.

The major optimization cycle is divided into secondary cycles with intermediate targets (η_{target}). The resizing approach in a secondary cycle is the uniform derivative approach of Ref. 4. The resizing factor of each element is

$$a_k \equiv \frac{w_{k_{\text{new}}}}{w_{k_{\text{old}}}} = \frac{\partial \eta}{\partial w_k}\Big/ T \tag{14}$$

where T and the associated a_k values are found iteratively such that the summation over all the resized elements gives

$$\eta + \sum_k \frac{\partial \eta}{\partial w_k}(a_k - 1) w_{k_{\text{old}}} = \eta_{\text{target}} \tag{15}$$

Once the resizing factors are defined, the finite-element model can be updated for repeated analysis (as is done in Ref. 4). The present method, however, allows additional efficient secondary cycles. A new secondary cycle starts with recalculating the derivatives of Eq. (11) with

$$[B]_{\text{new}} = [B]_{\text{old}} + \sum_k (a_k - 1)[K_{ee}^{(k)}] \tag{16}$$

The old η_{target} is now the starting value of η; a new η_{target} is defined and the resizing is repeated. After several secondary cycles, the NASTRAN model may be updated and a new major cycle performed if desired. The optimization procedure allows setting minimum and maximum limits to the accumulated resizing factors of each element. If any of the a_k values calculated by Eq. (14) violates its minimum or maximum limit, the value is fixed to meet the violated limit.

Numerical Example

A preliminary version of the Lavi wing has been used to demonstrate the method. The resized elements were those of the skins only. The analysis was done with antisymmetric boundary conditions. The structural and aerodynamic models were based on wing-fuselage-canard components with a wing tip missile. Forty elastic modes were taken into account. The rigid-body modes were annexed with unit rigid aileron rotation. The flight conditions were Mach 1.2 and sea level.

The driving parameter was chosen to be the ratio between the effectiveness of C_{L_δ} (η_1) and the effectiveness of C_{H_δ} (η_2). This ratio gives the effectiveness of rolling moment per unit hinge moment. This parameter is important because the aircraft roll performance at high speed is limited by maximum actuator-force capability. The accumulated resizing factors were limited to be minimum 1.0, to avoid violation of stress and minimum gage requirements, and maximum 1.4, to yield a smooth (practical) design.

The optimization process is depicted in Fig. 1. The starting value of the driving parameter is 85% of the target value. The first major cycle aimed to achieve the target value in 3 secondary cycles. Even though the structural changes in the first major cycle were relatively large, the updated value of the driving parameter, based on an analysis of the full NASTRAN model, was only 2.5% below the predicted value. A second major cycle was then performed in two steps to close the gap. In this cycle, the difference between the value predicted by the optimization and the actual value calculated directly from the NASTRAN update was negligible.

The accumulated resizing factors (rounded to one decimal digit values) for the upper skin are shown in Fig. 2 with similar results for the lower skin. Most of the resizing is in the wing torsion box, outboard of the main support fittings region where the skin is not effective. Other resized regions are in the outboard elevon, near the actuator horn connection, and at the wing tip, near the launcher connection to the wing. It should be noted that most parts of the elevons are not resized. Even though elevon stiffening would increase the rolling moment due to aileron deflection, it would increase even more the associated hinge moment and by this reduce the rolling moment per unit actuator force. This demonstrates the importance of considering the ratio of $C_{L_\delta}/C_{H_\delta}$ when actuator saturation may occur within the performance envelope.

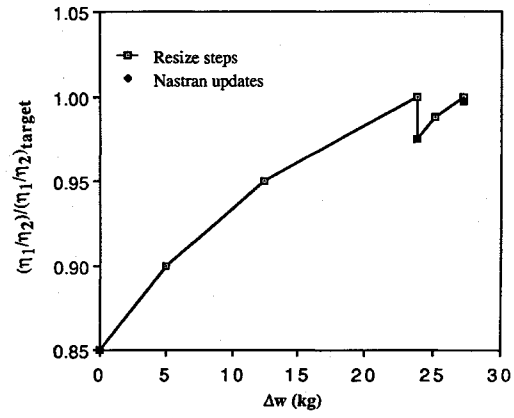

Fig. 1 Normalized driving parameter vs additional structural weight.

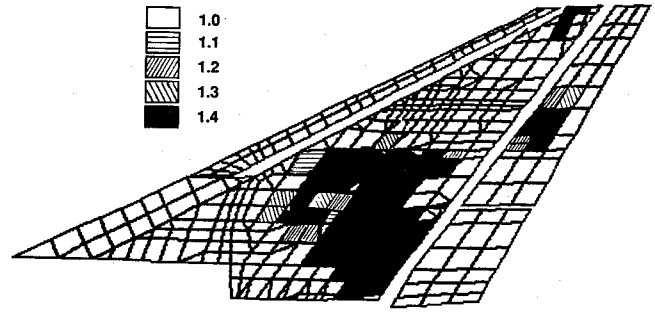

Fig. 2 Resizing factors in the upper skin of the wing.

References

[1]Wilkinson, K., Lerner, E., and Taylor, R. F., "Practical Design of Minimum Weight Aircraft Structures for Strength and Flutter Requirements," *Journal of Aircraft,* Vol. 13, Aug. 1976, pp. 614–624.

[2]Wilkinson, K., Markowitz, J., Lerner, E., George, D., and Batill, S. M., "FASTOP: A Flutter and Strength Optimization Program for Lifting-Surface Structures," *Journal of Aircraft,* Vol. 14, June 1977, pp. 581–587.

[3]Isakson, G., Pardo, H., Lerner, E., and Venkayya, V., "ASOP-3: A Program for the Optimum Design of Metallic and Composite Structures Subjected to Strength and Deflection Constraints," *Journal of Aircraft,* Vol. 15, July 1978, pp. 422–428.

[4]Lerner, E. and Markowitz, J., "An Efficient Structural Resizing Procedure for Meeting Static Aeroelastic Design Objectives," *Journal of Aircraft,* Vol. 16, Feb. 1979, pp. 65–71.

[5]Lerner, E., "The Application of Practical Optimization Techniques in the Preliminary Structural Design of a Forward-Swept Wing," *Collected Papers of the Second International Symposium on Aeroelasticity and Structural Dynamics,* DGLR Bericht 85-02, Aachen, West Germany, April 1985, pp. 381–393.

[6]Stirk, M. H., Hertz, T. J., and Weisshaar, T. A., "Aeroelastic Tailoring—Theory, Practice, Promise," *Journal of Aircraft,* Vol. 23, Jan. 1986, pp. 6–18.

[7]Sheena, Z. and Karpel, M., "Static Aeroelastic Analysis Using Aircraft Vibration Modes," *Collected Papers of the Second International Symposium on Aeroelasticity and Structural Dynamics,* DGLR Bericht 85-02, Aachen, West Germany, April 1985, pp. 229–232.

Finite-Surface Spline

Kari Appa*
Northrop Corporation,
Hawthorne, California

I. Introduction

In aeroelastic analyses by finite-element methods, different discretization procedures are employed to determine the structural and aerodynamic loads. To formulate the equations of motion, it is necessary to represent the equivalent air loads at the structural grid points and to represent the structural deflections at the aerodynamic grid points. Over the years, numerous schemes have been proposed to obtain these necessary transformations.[1–6] However, application of these methods frequently impose some restrictions on the format of the structural data, or the methods pose as inconveniences to the user. For example, Ref. 6 requires that the data be given along spanwise or chordwise lines, but structural layouts seldom have such a pattern. Reference 7 has presented an example illustrating that the infinite-surface spline of Harder and Desmarais[5] provides results within acceptable accuracy and user convenience without restriction. However, subsequent experience with the infinite-surface spline indicates that extrapolations to the edges of the planform from the interior structural grid points do not always appear to be reliable. An alternative approach using a network of rectangular grids and hermitian polynominals in each of the rectangular boxes was proposed in Ref. 8. Since no results are reported in this reference, there is very little to say about the success of this method.

The infinite plate-surface spline is appealing in its simplicity, since it has a closed-form solution. Because of observed limitations of the infinite plate, a finite uniform plate with the planform of the aerodynamic lifting surface suggests itself as an alternative with adequate simplicity and reliability. The present method employs uniform plate elements to represent a given planform by a number of quadrilateral or triangular bending elements. A set of constraint conditions using shape functions that are employed in the determination of the stiffness matrix of the plate element are established such that the deformed plate passes through the given data points. Subsequently, a mapping matrix relating displacements at structural and aerodynamic grid points are derived. This transformation matrix provides a general two-dimensional interpolation scheme not limited to the structural and aerodynamic interface, but also applicable to interpolate any smooth data, such as pressure, temperature, or strains.

Received July 28, 1988; revision received Sept. 7, 1988.

*Senior Technical Specialist, Dynamics and Loads Research Department, Aircraft Division.

II. Derivation of a Mapping Matrix

Consider m number of aerodynamic points at which the displacements and slopes are required in terms of structural displacements given at n points. To achieve this, a linear mapping matrix is developed employing the structural finite-element method, based on the minimum energy principle. In other words, the structure deforms to a unique surface that conforms to the given data points. Figure 1 shows a typical arrangement of a finite-element model of a given planform, as well as representative structural and aerodynamic data points, which may not have a regular arrangement or layout. The displacement w, in the z direction, and rotations (θ about the x axis, ϕ about the y axis) at any point (x,y) within an element, using the notations of Refs. 9 and 10, are given by

$$r = \Omega \rho \tag{1}$$

where

$$r = \begin{Bmatrix} w \\ \theta \\ \phi \end{Bmatrix} \tag{2}$$

$$\Omega = \begin{bmatrix} \omega \\ \omega_y \\ \omega_x \end{bmatrix} \tag{3}$$

$$\rho = \{ w_1\ \theta_1\ \phi_1 \ldots w_4\ \theta_4\ \phi_4 \} \tag{4}$$

in which ω is a (1×12) row matrix of the shape functions (e.g., Ref. 9) used to interpolate the displacements within a four-node quadrilateral element in terms of its nodal degrees of freedom ρ. The vector ρ can be related to the global displacement vector q by means of a Boolean connectivity matrix a.

For example, for the ith element

$$\rho_i = a_i\, q \tag{5}$$

Using Eq. (5) in Eq. (1), the displacement vector r_s for n structural constraint points (subscript s) can be written, after assembly, as

$$q_s = \Psi_s\, q \tag{6}$$

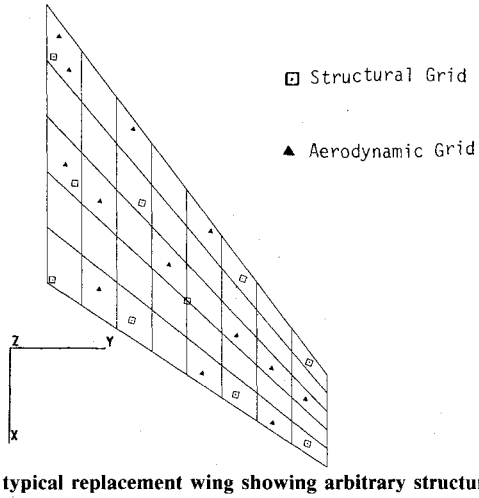

Fig. 1 A typical replacement wing showing arbitrary structural and aerodynamic grids.